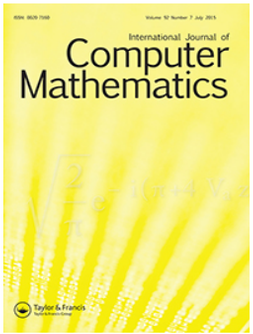

International Journal of Computer Mathematics

ISSN: 0020-7160 (Print) 1029-0265 (Online) Journal homepage: http://www.tandfonline.com/loi/gcom20

Inverse Sturm–Liouville problems with pseudospectral methods

H. Altundağ, C. Böckmann & H. Taşeli

To cite this article: H. Altundağ, C. Böckmann & H. Taşeli (2015) Inverse Sturm–Liouville problems with pseudospectral methods, International Journal of Computer Mathematics, 92:7, 1373-1384, DOI: 10.1080/00207160.2014.939646

To link to this article: http://dx.doi.org/10.1080/00207160.2014.939646

Accepted author version posted online: 01 Jul 2014.
Published online: 24 Jul 2014.

International Journal of Computer Mathematics, 2015
Vol. 92, No. 7, 1373–1384, http://dx.doi.org/10.1080/00207160.2014.939646

Inverse Sturm–Liouville problems with pseudospectral methods

H. Altundağ[a*,†], C. Böckmann[a] and H. Taşeli[b]

[a]*Institute of Mathematics, University of Potsdam, Am Neuen Palais 10, 14469 Potsdam, Germany;*
[b]*Department of Mathematics, Middle East Technical University, 06531 Ankara, Turkey*

(*Received 25 November 2013; revised version received 13 June 2014; accepted 20 June 2014*)

In this paper a technique to obtain a first approximation for singular inverse Sturm–Liouville problems with a symmetrical potential is introduced. The singularity, as a result of unbounded domain $(-\infty, \infty)$, is treated by considering numerically the asymptotic limit of the associated problem on a finite interval $(-L, L)$. In spite of this treatment, the problem has still an ill-conditioned structure unlike the classical regular ones and needs regularization techniques. Direct computation of eigenvalues in iterative solution procedure is made by means of pseudospectral methods. A fairly detailed description of the numerical algorithm and its applications to specific examples are presented to illustrate the accuracy and convergence behaviour of the proposed approach.

Keywords: regular and singular inverse Sturm–Liouville problems; pseudospectral method; condition number; regularization method

2010 AMS Subject Classifications: 31A25; 65F18

1. Introduction

Eigenvalue problems as well as inverse eigenvalue problems for differential equations are frequently encountered in practice in connection with physical and engineering applications [11,23]. The Sturm–Liouville problem (SLP), containing the canonical form of a second order differential equation

$$-y'' + q(x)y = \lambda y \tag{1}$$

is of particular importance, where $q(x)$ stands for a continuous real-valued function. The regular SLPs on a finite interval of x with appropriate homogeneous boundary conditions are relatively simpler than the singular problems on the whole real line $(-\infty, \infty)$. There are mainly two different lines of approaches to calculate the eigenvalues and eigenfunctions of singular SLPs for a given potential $q(x)$ [25]. Roughly speaking, in the first, a domain truncation is used where the singular SLP is approximated by a regular SLP over a finite interval $x \in [-L, L]$ with L sufficiently large [5,24,26,34,37]. The second type of methods is based on a series expansion of the solution via basis functions intrinsic to an infinite interval, such as appropriately weighted Hermite polynomials or sinc-functions [8,35]. Both approaches reduce the problem to a matrix-eigenvalue problem.

*Corresponding author. Email: huseyinaltundag@hitit.edu.tr
†Current address: Department of Mathematics, Hitit University, 19030 Çorum, Turkey.

On the other hand, inverse problems are much more involved than the direct problems, where the main question is to determine the potential q from eigenvalues, notably the celebrated works by Borg [7] and by Gel'fand and Levitan [17] stating the fundamental fact that two sets of data sequences are required to uniquely determine a potential. A quick introduction to regular inverse SLPs can be found in [10]. One approach is based on simple matrix methods. Another one consists of transforming the regular SLP to a hyperbolic Cauchy or Goursat problem [27,31]. A further type constructs particularly suitable functionals which one has to minimize in recovering the potential [9,30]. However, the recovery of $q(x)$ from spectral data is a difficult and ill-conditioned numerical problem. More recently a numerical approach based on Numerov's method was proposed by Andrew [3,4] to estimate the potential from eigenvalues by using asymptotic corrections, which offers significant advantages. Similar technique was also used in [1,6,16,18,21,22] to construct q with various initial data by means of Numerov's method and a boundary value method.

The ultimate goal of this study is to introduce an approach for solving inverse SLPs with a symmetric potential [18]

$$q(x) = q(-x), \tag{2}$$

on $x \in (-L, L)$, which also gives a first approximation for the singular problem over $(-\infty, \infty)$ for increasing L. Thus the paper presents a novel approach incorporated with regularization techniques. Some preliminaries for a pseudospectral discretization of a differential equation are given in Section 2. The inverse problem is formulated in Section 3, where the regularization process is also introduced. Section 4 deals with the construction of the algorithm and its numerical implementations. Section 5 concludes the paper with certain remarks.

2. Pseudospectral discretization of the direct problem

The basic idea behind a pseudospectral method is to approximate the solution of (1) by a weighted interpolant of the form

$$y(x) \approx p(x) = \sum_{j=0}^{N} \frac{\omega(x)}{\omega(x_j)} \phi_j(x) y_j, \quad y_j := y(x_j) \tag{3}$$

in which the x_j are distinct interpolation nodes, $\omega(x)$ denotes a weight function, and the $\phi_j(x)$ are interpolating functions with the property $\phi_j(x_k) = \delta_{jk}$ for $j, k = 0, 1, \ldots, N$, where δ_{jk} stands for Kronecker's delta. The interpolant $p(x)$ and the exact solution $y(x)$ agree, at least, at the nodes. The choices of $\phi_j(x)$ classifies the pseudospectral methods as polynomial (Chebyshev, Hermite, Laguerre) and non-polynomial (sinc, Fourier) cases.

We may also approximate the derivative $y'(x)$ by making use of the derivative $p'(x)$ of the interpolant in Equation (3). Furthermore, the derivative values at the same $N + 1$ nodes x_j can be determined with the help of a differentiation matrix defined by

$$\boldsymbol{D}^{(1)} := [d_{kj}^{(1)}] = \left[\frac{\mathrm{d}}{\mathrm{d}x} \left(\frac{\omega(x)}{\omega(x_j)} \phi_j(x) \right) \Big|_{x=x_k} \right] \tag{4}$$

for $j, k = 0, 1, \ldots, N$, leading to the system

$$y'_k := y'(x_k) \approx p'(x_k) = \sum_{j=0}^{N} d_{kj}^{(1)} y_j, \quad k = 0, 1, \ldots, N \tag{5}$$

which is expressible, in matrix–vector form, as

$$\boldsymbol{y}^{(1)} = \boldsymbol{D}^{(1)}\boldsymbol{y}, \tag{6}$$

where $\boldsymbol{y}^{(1)} = [y_0', y_1', \ldots, y_N']^{\mathrm{T}}$ and $\boldsymbol{y} = [y_0, y_1, \ldots, y_N]^{\mathrm{T}}$ are the vectors whose entries contain, respectively, approximate values of the derivative $y'(x)$ and the exact values of $y(x)$ at the grid points. Higher order derivatives of the function $y(x)$ at the grid points can be approximated by the same way [37,38].

In this work, we employ the non-polynomial Fourier (or trigonometric) pseudospectral method (FPM), which assumes the equally spaced grid points on the interval $[0, 2\pi]$. Thus we first convert the original interval $[-L, L]$ of x into $[0, 2\pi]$ by the scaling transformation

$$\xi = \frac{\pi x}{L} + \pi, \quad \xi \in [0, 2\pi] \tag{7}$$

so that the SLP in Equation (1) subject to Dirichlet boundary conditions $y(\pm L) = 0$ becomes

$$-\frac{\mathrm{d}^2 y}{\mathrm{d}\xi^2} + v(\xi)y = \mathcal{E}y, \quad y(0) = y(2\pi) = 0, \tag{8}$$

where

$$v(\xi) = \left(\frac{L}{\pi}\right)^2 q\left(\frac{L(\xi - \pi)}{\pi}\right) \quad \text{and} \quad \mathcal{E} = \left(\frac{L}{\pi}\right)^2 \lambda \tag{9}$$

denote the modified potential in ξ and the new eigenvalue parameter $\mathcal{E}$, respectively. Now the modified potential is symmetric about the line $\xi = \pi$, i.e. $v(\xi) = v(2\pi - \xi)$.

In FPM, the weight is unity, and the interpolation functions are the so-called periodic sinc functions conventionally taken as

$$\phi_j(\xi) = \frac{1}{N}\begin{cases} \sin\left[\dfrac{N(\xi - \xi_j)}{2}\right]\cot\left[\dfrac{(\xi - \xi_j)}{2}\right] & \text{for } N \text{ even}, \\ \sin\left[\dfrac{N(\xi - \xi_j)}{2}\right]\csc\left[\dfrac{(\xi - \xi_j)}{2}\right] & \text{for } N \text{ odd}, \end{cases} \tag{10}$$

where the grid points $\xi_j = 2\pi j/N$ for $j = 0, 1, \ldots, N$. At the point $\xi = \xi_j$, we define $\phi_j(\xi_j) = 1$ as the limit of indeterminate form $0 \cdot \infty$. The use of sinc functions seems to be reasonable when we keep in mind the periodic nature of solutions of (8) under Dirichlet conditions.

Then taking the first derivative of $\phi_j(\xi)$ and evaluating at $\xi = \xi_k$ we see, from Equation (4), that the elements of the first order differentiation matrix are expressible explicitly as

$$d_{kj}^{(1)} = \frac{1}{2}\begin{cases} 0 & \text{if } k = j \\ (-1)^{k-j}\cot\left[\dfrac{(k-j)\pi}{N}\right] & \text{if } k \neq j \end{cases}$$

for N even, and

$$d_{kj}^{(1)} = \frac{1}{2}\begin{cases} 0 & \text{if } k = j \\ (-1)^{k-j}\csc\left[\dfrac{(k-j)\pi}{N}\right] & \text{if } k \neq j \end{cases}$$

for N odd. It should be noted here that the diagonal element $d_{jj}^{(1)} = 0$ has been determined again by a limiting procedure.

Similarly, we have derived the elements of the second order differentiation matrix

$$d_{kj}^{(2)} = -\frac{1}{12}\begin{cases} N^2+2 & \text{if } k=j \\ 6(-1)^{k-j}\csc^2\left[\dfrac{(k-j)\pi}{N}\right] & \text{if } k\neq j \end{cases} \tag{11}$$

for N even and

$$d_{kj}^{(2)} = -\frac{1}{12}\begin{cases} N^2+1 & \text{if } k=j \\ 6(-1)^{k-j}\csc\left[\dfrac{(k-j)\pi}{N}\right]\cot\left[\dfrac{(k-j)\pi}{N}\right] & \text{if } k\neq j \end{cases} \tag{12}$$

for N odd. Therefore, the second order derivative values $y_k'' := y''(\xi_k)$ at the grid points may be calculated approximately by a matrix–vector product

$$\boldsymbol{y}^{(2)} = \boldsymbol{D}^{(2)}\boldsymbol{y}, \tag{13}$$

where $\boldsymbol{y}^{(2)} = [y_0'', y_1'', \ldots, y_N'']^{\mathrm{T}}$ and $\boldsymbol{D}^{(2)} := [d_{kj}^{(2)}] = [\phi_j''(\xi_k)]$. Now if we propose a trial solution

$$y(\xi) = \sum_{j=0}^{N} \phi_j(\xi) y_j \tag{14}$$

with $\phi_j(\xi)$ in Equation (10), the discrete representation of (8) via FPM is given by

$$(-\boldsymbol{D}^{(2)} + \boldsymbol{V})\boldsymbol{y} = \mathcal{E}\boldsymbol{y}, \tag{15}$$

where $\boldsymbol{V} = \mathrm{diag}[v(\xi_0), v(\xi_1), \ldots, v(\xi_N)]$ is the diagonal matrix generated by the modified potential in Equation (9). Note that $\boldsymbol{D}^{(2)}$ and $\boldsymbol{V}$ are both symmetric and square matrices of order $N+1$. However since Dirichlet boundary conditions in Equation (8) require simply that $y_0 = y_N = 0$ and that deleting both first and the last rows and columns of the coefficient matrix, the system is reduced to a matrix eigenvalue problem of order $N-1$. As a result, the potential values $v(0) = v(\xi_0)$ and $v(2\pi) = v(\xi_N)$ at the end points of the interval $[0, 2\pi]$ do not play any role in this algorithm.

3. The inverse problem

The inverse problem concerns with finding an M-vector whose components give an approximation to a symmetric potential $q(x)$ at grid points in the domain of interest under the assumption that the first M eigenvalues $\lambda_1 \leq \lambda_2 \leq \cdots \leq \lambda_M$ of (1) are definite. In fact, we initially recover the modified potential $v(\xi)$ in the transformed SLP (8) by means of the rescaled eigenvalues $\mathcal{E}_1, \mathcal{E}_2, \ldots, \mathcal{E}_M$, which are calculated immediately by formula (9) for the known set of λ_m for $m = 1, 2, \ldots, M$ and a prescribed boundary parameter L. In this process we consider a nonlinear vector equation in the form

$$\boldsymbol{T}(\boldsymbol{v}) = \boldsymbol{0}, \tag{16}$$

which may be solved iteratively by Newton's method, where the vector $\boldsymbol{v}$ represents the potential function at M grid points, i.e. $\boldsymbol{v} = [v_1, \ldots, v_m, \ldots, v_M]^{\mathrm{T}}$ with $v_m := v(\xi_m)$, and mth component $T_m(\boldsymbol{v})$ of the vector $\boldsymbol{T}(\boldsymbol{v})$ carries the difference

$$T_m(\boldsymbol{v}) = \mathcal{E}_m(\boldsymbol{v}) - \mathcal{E}_m, \quad m = 1, 2, \ldots, M \tag{17}$$

so that the L_2 norm $\|\boldsymbol{T}(\boldsymbol{v})\|$ defines a residual for the eigenvalues. Here, $\mathcal{E}_m(\boldsymbol{v})$ denotes the mth eigenvalue of (15) to be calculated as a function of iterated potentials starting with a prescribed

initial potential vector, say $\boldsymbol{v} = \boldsymbol{v}^0 = [v_1^0, \ldots, v_M^0]^{\mathrm{T}}$. Then it is appropriate to use the FPM described in Section 2 with $N = 2M + 1$ for solving

$$(-\boldsymbol{D}^{(2)} + \boldsymbol{V}^k)\boldsymbol{y}^k = \mathcal{E}(\boldsymbol{v}^k)\boldsymbol{y}^k, \quad k = 0, 1, \ldots, \tag{18}$$

where $\boldsymbol{V}^k = \mathrm{diag}[v(\xi_0), v(\xi_1), \ldots, v(\xi_M), v(\xi_M), \ldots, v(\xi_1), v(\xi_0)]$ is constructed for each iteration step k, keeping in mind the symmetry of the potential. Recalling that the first and last rows and columns of the coefficient matrix are omitted to satisfy Dirichlet conditions, we have in practice a $2M \times 2M$ system in Equation (18). Clearly, we need only the first M eigenvalues to define $T_m(\boldsymbol{v})$ in Equation (17) for $\boldsymbol{v} = \boldsymbol{v}^k$. It should also be noted that the entries of the vector $\boldsymbol{v}$ so defined, now, stand for the approximate values of the potential at $\xi_m = 2m\pi/(2M + 1)$ in $(0, \pi)$, excluding the end points due to the nature of the FPM.

If we assume that $\boldsymbol{T}(\boldsymbol{v})$ is differentiable with respect to $\boldsymbol{v}$, we define the so-called Jacobian matrix

$$\boldsymbol{A}(\boldsymbol{v}) = \frac{\partial \boldsymbol{T}}{\partial \boldsymbol{v}} := [a_{mn}]_{M\times M} = \left[\frac{\partial T_m}{\partial v_n}\right]_{M\times M} = \left[\frac{\partial \mathcal{E}_m}{\partial v_n}\right]_{M\times M} \tag{19}$$

whose generic element a_{mn} is $\partial \mathcal{E}_m/\partial v_n$. Then Newton's method for Equation (16) leads to the system $\boldsymbol{T}(\boldsymbol{v}^0) + \boldsymbol{A}(\boldsymbol{v}^0)(\boldsymbol{v} - \boldsymbol{v}^0) = \boldsymbol{0}$, from which we have

$$\boldsymbol{T}(\boldsymbol{v}^k) + \boldsymbol{A}(\boldsymbol{v}^k)(\boldsymbol{v}^{k+1} - \boldsymbol{v}^k) = \boldsymbol{0} \tag{20}$$

on generalizing the notation [12]. Now it is customary to introduce the Newton's correction $\Delta\boldsymbol{v}^k = \boldsymbol{v}^k - \boldsymbol{v}^{k+1}$ as the unknown vector and solve the system

$$\boldsymbol{A}(\boldsymbol{v}^k)\Delta\boldsymbol{v}^k = \boldsymbol{T}(\boldsymbol{v}^k) \tag{21}$$

in order to update the potential vector by

$$\boldsymbol{v}^{k+1} = \boldsymbol{v}^k - \Delta\boldsymbol{v}^k, \quad k = 0, 1, \ldots \tag{22}$$

at each iteration. To this end, it remains only to evaluate the elements a_{mn} of the Jacobian matrix [2,21]. It can be shown, after some algebra, that the derivation of a_{mn} is accomplished by the simple formula

$$a_{mn} = 2(y_{n;m})^2, \quad m, n = 1, 2, \ldots, M \tag{23}$$

for every iteration step k, where the $y_{n;m}$ denote the first M non-zero entries of the mth eigenvector $\boldsymbol{y}_m = [0, y_{1;m}, y_{2;m}, \ldots, y_{n;m}, \ldots, y_{M;m}, y_{M+1;m}, \ldots, y_{2M;m}, 0]^{\mathrm{T}}$ of (18).

3.1 *Newton–Tikhonov–Phillips regularization*

The linear system in Equation (21) cannot be solved for $\Delta\boldsymbol{v}^k$ directly by taking the inverse of the Jacobian matrix due to its ill-conditioned structure. The condition number defined by $\|\boldsymbol{A}^{-1}(\boldsymbol{v})\|\|\boldsymbol{A}(\boldsymbol{v})\|$ is a measure of ill-conditioning, which may be taken here as the ratio of the largest and the smallest singular values of the Jacobian matrix. Indeed it is shown, from Table 1, that such ratios and, hence, the condition numbers of $\boldsymbol{A}(\boldsymbol{v}^k)$ increase rapidly as k increases. Therefore, we have to use a regularization technique to cope with this problem. In other words, the nonlinear vector equation (16) will be solved by an inexact Newton method, which consists of two parts [20,28,29]. The first part is the outer Newton iteration which updates the current iterate. The second part is called the inner scheme providing updates by the approximate solution of a local linear version of (16) in Equation (21), where a regularization is needed. So our objective is

Table 1. The largest and smallest singular values of the Jacobian matrix $\boldsymbol{A}(\boldsymbol{v}^k)$ of order $M = 14$ in the first five iterations, for the harmonic oscillator in Equation (27) with $L = 7$.

1. Iteration	2. Iteration	3. Iteration	4. Iteration	5. Iteration
1.0400531126	1.0559558703	1.1145072672	1.1537342403	1.1735723266
0.0062072726	0.0046273881	0.0000153561	0.0000003699	0.0000000002

to approximate the ill-conditioned system (21) of the inner scheme by a suitable well-conditioned one.

A general representation of a linear regularization method is described by

$$\Delta \boldsymbol{v}^k \approx \Delta \boldsymbol{v}_\alpha^k = g_\alpha(\boldsymbol{A}^{\mathrm{T}}(\boldsymbol{v}^k)\boldsymbol{A}(\boldsymbol{v}^k))\boldsymbol{A}^{\mathrm{T}}(\boldsymbol{v}^k)\boldsymbol{T}(v^k) \tag{24}$$

in which g_α stands for a piecewise continuous filter function with a regularization parameter $\alpha > 0$. For example, the historical Tikhonov–Phillips (TP) regularization

$$g_\alpha(\boldsymbol{A}^{\mathrm{T}}(\boldsymbol{v}^k)\boldsymbol{A}(\boldsymbol{v}^k)) = [\boldsymbol{A}^{\mathrm{T}}(\boldsymbol{v}^k)\boldsymbol{A}(\boldsymbol{v}^k) + \alpha \boldsymbol{I}]^{-1}$$

is obtained, when $g_\alpha(\sigma_m^2) = (\sigma_m^2 + \alpha)^{-1}$, where the σ_m denote the singular values of the Jacobian matrix for $m = 1, 2, \ldots, M$. The purpose of the filter is to damp or filter out unwanted contributions resulting from the small singular values. On the other hand, the generalized TP regularization reads as

$$\Delta \boldsymbol{v}_\alpha^k = [\boldsymbol{A}^{\mathrm{T}}(\boldsymbol{v}^k)\boldsymbol{A}(\boldsymbol{v}^k) + \alpha \boldsymbol{D}^{\mathrm{T}}\boldsymbol{D}]^{-1}\boldsymbol{A}^{\mathrm{T}}(\boldsymbol{v}^k)\boldsymbol{T}(\boldsymbol{v}^k) \tag{25}$$

in which the identity matrix $\boldsymbol{I}$ is replaced by $\boldsymbol{D}^{\mathrm{T}}\boldsymbol{D}$, where $\boldsymbol{D}$ is some differentiation matrix [13].

Let $\{\sigma_m; \boldsymbol{u}_m, \boldsymbol{w}_m\}$ be the singular system associated with $\boldsymbol{A}(\boldsymbol{v}^k)$ such that $\boldsymbol{A}(\boldsymbol{v}^k)\boldsymbol{u}_m = \sigma_m \boldsymbol{w}_m$. Under the additional assumptions that $\|\boldsymbol{D}^{-1}\| \leq 1/\beta$ and $\boldsymbol{D}^{\mathrm{T}}\boldsymbol{D}\Delta\boldsymbol{v}^k = \sum_{m=1}^{M} \beta_m^2 \langle \Delta \boldsymbol{v}^k, \boldsymbol{u}_m\rangle \boldsymbol{u}_m$ with $\{\beta_k\} \subset [\beta, \|\boldsymbol{D}\|]$ hold, it is shown that the inner scheme may be updated by

$$\Delta \boldsymbol{v}_\alpha^k = \sum_{m=1}^{M} \sigma_m g_\alpha(\sigma_m^2)\langle \boldsymbol{T}(v^k), \boldsymbol{w}_m\rangle \boldsymbol{u}_m \tag{26}$$

with $g_\alpha(\sigma_m^2) = (\sigma_m^2 + \alpha\beta_m^2)^{-1}$. The influence of $\boldsymbol{D}$ is obvious. The stronger summands are damped by larger β values whereas in case of $\boldsymbol{D} = \boldsymbol{I}$ all components are treated uniformly. In a sense such a generalization allows us to penalize non-smooth *solutions*. By numerical simulations, the second order Hermite differentiation matrix [15] is employed here as a penalizing matrix.

To determine a suitable regularization parameter α, we prefer to make use of the heuristic *L-Curve* method since it is stable and practical. According to this method, one can plot the logarithms of the constraint $\|\boldsymbol{D}\Delta\boldsymbol{v}_\alpha^k\|$ versus the norm of residual $\|\boldsymbol{A}(\boldsymbol{v}^k)\Delta\boldsymbol{v}_\alpha^k - \boldsymbol{T}(\boldsymbol{v}^k)\|$ for various values of the parameter α. Such a parametric curve has typically an *L-shaped* picture with a corner point at which the *best* possible regularization parameter is reached in each iteration. To this end, the curvature of the curve whose maximum identifies the corner, may be used (Figure 1). More on the *L-Curve* method can be found by perusing the literature, see for example [19,36] and references therein.

On the other hand, we control the outer scheme by means of the iteration number k. For this purpose, we introduce a tolerance threshold ϵ, typically like $\epsilon = 10^{-6}$, and require that $\|\Delta\boldsymbol{v}^k\| < \epsilon\|\boldsymbol{v}^k\|$. Nevertheless, we also set a maximum number of iterations $K_{\max} = 50$ to terminate the procedure in any case.

It is worth mentioning, in practice, that the initial data, specifically the input eigenvalues λ_m, may contain several errors in many times, what is called the *noisy* data λ_m^δ say. As a result of

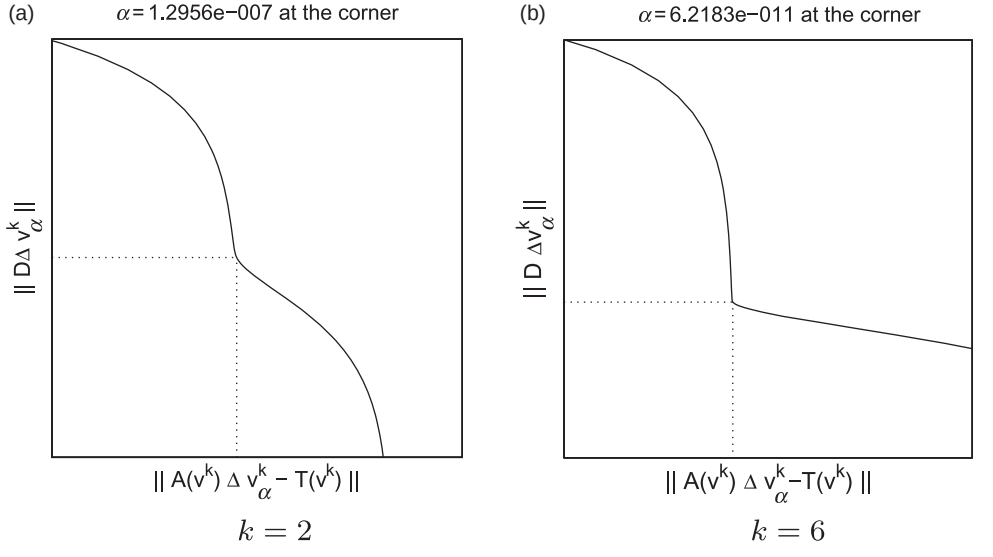

Figure 1. *L-Currves* for two typical iterations. (a) k = 2 and (b) k = 6.

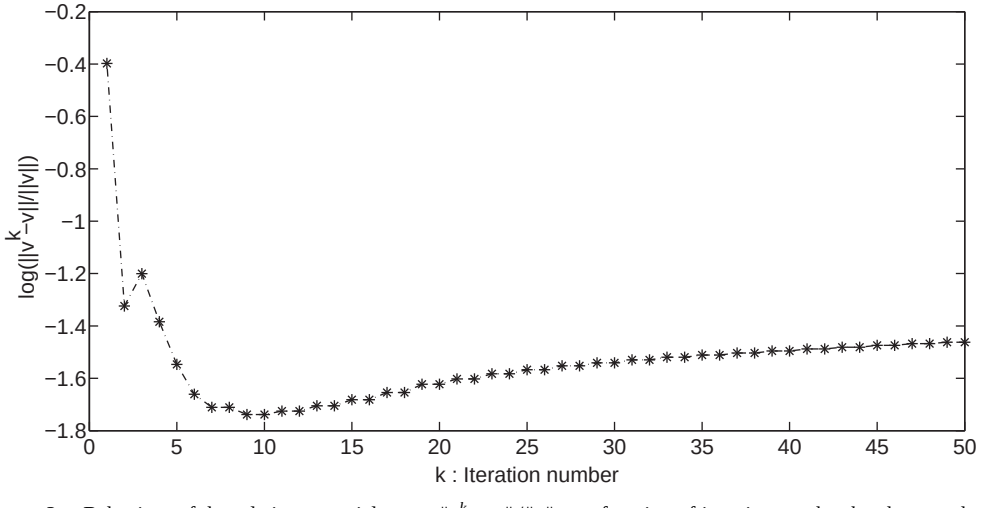

Figure 2. Behaviour of the relative potential errors $\|\boldsymbol{v}^k - \boldsymbol{v}\|/\|\boldsymbol{v}\|$ as a function of iteration number k, where we have used noisy data with %19 noise for the harmonic oscillator when $L = 9$ and $M = 26$.

the propagated data error, the increment of k beyond a certain size of iteration, say K_δ, is useless for a further treatment of the problem in question (Figure 2). Actually, if a noise level δ, which has been measured somehow, is known then Morozov's discrepancy principle may be taken into account to terminate outer Newton's iterations in such a way that

$$\|\boldsymbol{T}^\delta(\boldsymbol{v}^{K_\delta})\| < \tau\delta < \|\boldsymbol{T}^\delta(\boldsymbol{v}^k)\|, \quad k = 1, 2, \ldots, K_\delta - 1,$$

where the elements of the vector $\boldsymbol{T}^\delta(\boldsymbol{v})$ is defined by Equation (17), i.e. $T_m^\delta(\boldsymbol{v}) = \mathcal{E}_m(\boldsymbol{v}) - \mathcal{E}_m^\delta$, and $\tau > 0$ is a prescribed scaling parameter [14]. It is shown, from Figure 2, that the threshold iteration number so defined is about $K_\delta = 10$.

4. The algorithm and numerical results

The algorithmic structure of the proposed method and numerical results for two illustrative examples are presented here.

4.1 *Algorithm*

The computation of a symmetric potential $q(x)$ from one sequence of eigenvalues for the SLP on $x \in [-L, L]$ as a function of the boundary parameter L.

Input: Boundary parameter L; The first M eigenvalues λ_m of the SLP; The maximum number $K_{\max}$ of iterations k; Tolerance threshold ϵ (or, alternatively, $\tau\delta$ in a noisy case provided some noise level δ is known)

(1) Transform the domain of the problem from $x \in [-L, L]$ to $\xi \in [0, 2\pi]$ and find the rescaled eigenvalues $\mathcal{E}_m$ from Equation (9).
(2) Specify the grid points $\xi_m = 2m\pi/(2M+1)$ in the half interval $(0, \pi)$ for $m = 1, 2, \ldots, M$.
(3) Choose the initial potential vector $\boldsymbol{v}^0 = [v_1^0, \ldots, v_M^0]^{\mathrm{T}}$ and set $k = 1$.
(4) Repeat until $\|\Delta \boldsymbol{v}^{k-1}\| < \epsilon \|\boldsymbol{v}^{k-1}\|$ or $\|\boldsymbol{T}^{\delta}(\boldsymbol{v}^{k-1})\| < \tau\delta$ or $k \geq K_{\max}$.
   (a) Solve Equation (18) for $\mathcal{E}(\boldsymbol{v}^{k-1})$ and $\boldsymbol{y}^{k-1}$.
   (b) Construct Jacobian matrix $\boldsymbol{A}(\boldsymbol{v}^{k-1}) = [a_{mn}^{k-1}]$ by Equation (23) and $\boldsymbol{T}(\boldsymbol{v}^{k-1}) = [T_m(\boldsymbol{v}^{k-1})]$ by Equation (17).
   (c) Approximate $\Delta \boldsymbol{v}^{k-1}$ by TP regularization in Equation (26).
   (d) Update potential vector by $\boldsymbol{v}^k = \boldsymbol{v}^{k-1} - \Delta \boldsymbol{v}^{k-1}$.
   (e) Replace $\boldsymbol{v}^{k-1}$ by $\boldsymbol{v}^k$ and k by $k+1$.

Output: The potential vector $\boldsymbol{v} = [v(\xi_1), v(\xi_2), \ldots, v(\xi_M)]^{\mathrm{T}}$ on $\xi \in (0, \pi)$. Use symmetry for an extension to $(0, 2\pi)$. Then return back to the original variable $x \in [-L, L]$ by Equation (7).

4.2 *Numerical examples*

We first attempt to reconstruct the quantum mechanical harmonic oscillator, where

$$q(x) = x^2 \tag{27}$$

having exact analytical solutions on $x \in (-\infty, \infty)$. Indeed, the first M eigenvalues of the direct singular problem, determined by the simple formula $\lambda_m = 2m + 1$, are used as input data of the present algorithm. This is motivated by the fact that the low lying state eigenvalues of the harmonic oscillator, namely the first 25–30 of them, may be computed by the direct problem on $x \in [-L, L]$ to an accuracy more than 20 decimal points, when L is about 10 [32,33]. To be more specific, the eigenvalues of the Dirichlet boundary value problem are decreasing as L increases and give upper bounds to those of the singular problem, so that a systematic investigation on the boundary parameter L provides a very good check on the accuracy of the results [34]. Accordingly, we repeat the calculations for successive values of L such as $L = 7, 8, 9$ and 10 to deduce numerically the nature of convergence of the regular inverse problem in the approximation of singular potential $q(x) = x^2$.

Tables 2 and 3 introduce the relative errors in the potential as functions of L and M. We also include the eigenvalue residuals in these tables as another indication for convergence. On the other hand, the convergence rate of Newton's method in Section 3 is linear, which may be seen from explanatory calculations in Table 4 and from Figure 3(a). The linear convergence is inevitable since the elements a_{mn} in Equation (23) of the Jacobian matrix can only be evaluated in terms of approximate eigenvectors $\boldsymbol{y}^k$ of (18) for each k.

Table 2. Eigenvalue residuals $\|\boldsymbol{T}(\boldsymbol{v})\|$ and relative potential errors $\|\boldsymbol{v}^K - \boldsymbol{v}\|/\|\boldsymbol{v}\|$ at $L = 7$ and $L = 8$, as a function of M for the harmonic oscillator, where K is the last iteration number.

$L = 7$			$L = 8$		
M	$\|\boldsymbol{T}(\boldsymbol{v})\|$	$\|\boldsymbol{v}^K - \boldsymbol{v}\|/\|\boldsymbol{v}\|$	M	$\|\boldsymbol{T}(\boldsymbol{v})\|$	$\|\boldsymbol{v}^K - \boldsymbol{v}\|/\|\boldsymbol{v}\|$
12	1.845×10^{-2}	1.247	17	2.271×10^{-4}	1.834×10^{-1}
13	1.104×10^{-3}	1.799×10^{-1}	18	2.903×10^{-5}	6.028×10^{-2}
14	2.311×10^{-3}	2.355×10^{-1}	19	3.716×10^{-6}	4.841×10^{-2}
15	7.968×10^{-4}	5.353×10^{-2}	20	9.920×10^{-4}	1.770×10^{-1}
16	1.766×10^{-3}	6.573×10^{-2}	21	1.025×10^{-4}	3.677×10^{-2}
17	2.501×10^{-3}	1.016×10^{-1}	22	3.083×10^{-5}	6.315×10^{-2}
18	5.388×10^{-3}	1.365×10^{-1}	23	1.321×10^{-3}	8.660×10^{-2}

Table 3. Eigenvalue residuals $\|\boldsymbol{T}(\boldsymbol{v})\|$ and relative potential errors $\|\boldsymbol{v}^K - \boldsymbol{v}\|/\|\boldsymbol{v}\|$ at $L = 9$ and $L = 10$, as a function of M for the harmonic oscillator, where K is the last iteration number.

$L = 9$			$L = 10$		
M	$\|\boldsymbol{T}(\boldsymbol{v})\|$	$\|\boldsymbol{v}^K - \boldsymbol{v}\|/\|\boldsymbol{v}\|$	M	$\|\boldsymbol{T}(\boldsymbol{v})\|$	$\|\boldsymbol{v}^K - \boldsymbol{v}\|/\|\boldsymbol{v}\|$
22	2.975×10^{-5}	1.709×10^{-1}	27	4.696×10^{-5}	8.278×10^{-2}
23	4.109×10^{-6}	8.258×10^{-2}	28	1.134×10^{-5}	5.952×10^{-2}
24	1.075×10^{-6}	5.488×10^{-2}	29	2.830×10^{-6}	5.929×10^{-2}
25	1.078×10^{-7}	5.499×10^{-2}	30	4.422×10^{-6}	5.127×10^{-2}
26	1.627×10^{-6}	5.040×10^{-2}	31	1.161×10^{-6}	5.693×10^{-2}
27	3.125×10^{-5}	6.312×10^{-2}	32	6.433×10^{-6}	4.034×10^{-2}
28	8.036×10^{-6}	1.014×10^{-1}	33	9.452×10^{-6}	5.503×10^{-2}

Table 4. Relative errors with respect to L_2 and L_∞ norms for the modified potential vector in the case of harmonic oscillator as a function of iteration number k, where $L = 8$ and $M = 21$.

k	$\|\boldsymbol{v}^k - \boldsymbol{v}\|_2/\|\boldsymbol{v}\|_2$	$\|\boldsymbol{v}^k - \boldsymbol{v}\|_\infty/\|\boldsymbol{v}\|_\infty$
0	4.6798×10^{-1}	3.2500×10^{-1}
1	1.3510×10^{-1}	1.4554×10^{-1}
2	3.8651×10^{-2}	7.6312×10^{-2}
3	2.3898×10^{-2}	4.7234×10^{-2}
4	2.1068×10^{-2}	4.0654×10^{-2}
5	2.0102×10^{-2}	3.8310×10^{-2}
6	1.9631×10^{-2}	3.7142×10^{-2}

Another important remark is that the choice of an initial potential $q^0(x)$ has a vital role in this process, which is typical for almost all algorithms in solving an inverse SLP. By numerical experiments, we observe that the best converged results can be obtained with an initial potential proportional virtually to the exact one, like $q^0(x) \propto \kappa_1 q(x) + \kappa_2$, where κ_1 is about 0.5 in the classical harmonic oscillator case. The range of the second parameter κ_2 is wider, typically between 0 and 100. Furthermore, the number of eigenvalues to be served is approximately $M = 30$. Hence, Figure 3(b) demonstrates the reconstructed harmonic oscillator potential in this way.

As a second example, we apply our algorithm to reconstruct a symmetric double well potential (SDWP)

$$q(x) = a_4 x^4 - a_2 x^2 + a_0, \quad a_4, a_2 > 0 \tag{28}$$

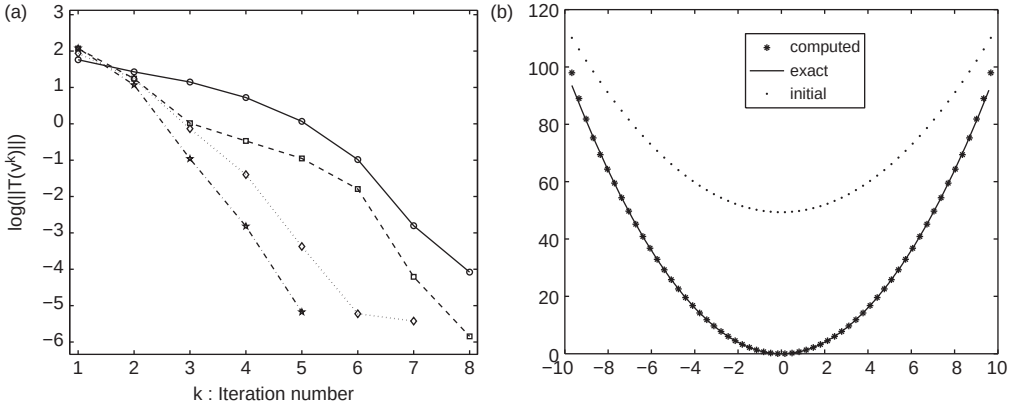

Figure 3. (a) Convergence behaviour of eigenvalue residuals; (b) reconstructed harmonic oscillator potential $q(x)$. (a) Convergence of eigenvalue residuals $\|\boldsymbol{T}(\boldsymbol{v}^k)\|$ as a function of k. Solid line ($L = 7, M = 14$), dashed line ($L = 8, M = 19$), dotted line ($L = 9, M = 25$), and dashed-dotted line ($L = 10, M = 31$) and (b) reconstructed potential ($L = 10, M = 31$).

Table 5. Eigenvalue residuals $\|\boldsymbol{T}(\boldsymbol{v})\|$ and relative potential errors $\|\boldsymbol{v}^K - \boldsymbol{v}\|/\|\boldsymbol{v}\|$ at $L = 5$, $L = 5.5$ and $L = 6$, as a function of M for the SDWP, where K is the last iteration number.

$L = 5$			$L = 5.5$			$L = 6$		
M	$\|\boldsymbol{T}(\boldsymbol{v})\|$	$\|\boldsymbol{v}^K - \boldsymbol{v}\|/\|\boldsymbol{v}\|$	M	$\|\boldsymbol{T}(\boldsymbol{v})\|$	$\|\boldsymbol{v}^K - \boldsymbol{v}\|/\|\boldsymbol{v}\|$	M	$\|\boldsymbol{T}(\boldsymbol{v})\|$	$\|\boldsymbol{v}^K - \boldsymbol{v}\|/\|\boldsymbol{v}\|$
20	4.494×10^{-5}	1.299×10^{-1}	30	1.591×10^{-3}	1.074×10^{-1}	47	1.570×10^{-4}	1.045×10^{-1}
21	3.851×10^{-5}	1.244×10^{-1}	31	6.496×10^{-5}	1.251×10^{-1}	48	2.817×10^{-6}	6.836×10^{-2}
22	4.316×10^{-5}	1.155×10^{-1}	32	7.480×10^{-5}	7.364×10^{-2}	49	1.994×10^{-4}	9.079×10^{-2}
23	3.673×10^{-5}	1.014×10^{-1}	33	5.102×10^{-5}	8.740×10^{-2}	50	8.065×10^{-5}	4.879×10^{-2}
24	2.414×10^{-4}	8.532×10^{-2}	34	2.803×10^{-5}	6.409×10^{-2}	51	5.751×10^{-5}	5.830×10^{-2}
25	1.074×10^{-3}	7.558×10^{-2}	35	1.656×10^{-4}	8.728×10^{-2}	52	1.217×10^{-4}	4.068×10^{-2}
26	2.448×10^{-3}	5.658×10^{-2}	36	3.709×10^{-4}	6.064×10^{-2}			
27	1.965×10^{-2}	1.675×10^{-1}	37	9.085×10^{-5}	5.298×10^{-2}			

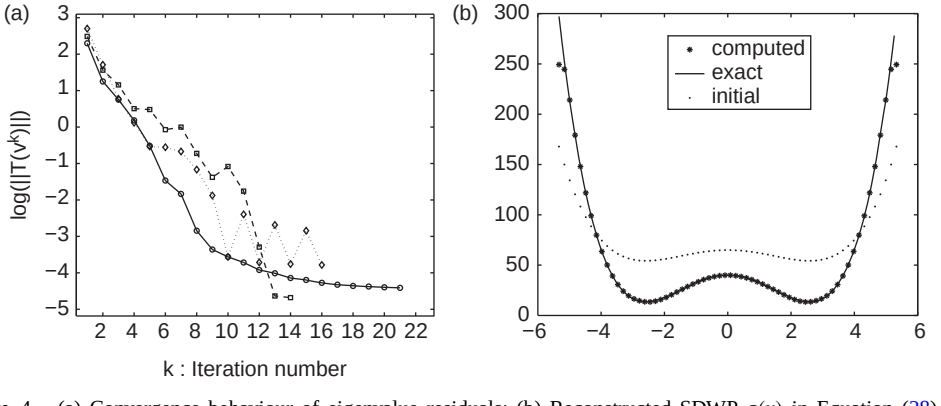

Figure 4. (a) Convergence behaviour of eigenvalue residuals; (b) Reconstructed SDWP $q(x)$ in Equation (28). (a) Convergence of eigenvalue residuals $\|\boldsymbol{T}(\boldsymbol{v}^k)\|$ as a function of k. Solid line ($L = 5$, $M = 21$), dashed line ($L = 5.5$, $M = 32$) and dotted line ($L = 6$, $M = 49$) and (b) Reconstructed potential ($L = 5.5$, $M = 32$).

the lower eigenvalues of which are closely bunched in pairs if the two wells are sufficiently separated, i.e. when $a_4/a_2 \ll 1$. In this case, the singular direct problem on $x \in (-\infty, \infty)$ possesses a nearly degenerate spectrum. We deal here with a specific SDWP with the coefficients

$a_4 = 0.6$, $a_2 = 8$ and $a_0 = 40$, whose first eight eigenvalues are nearly degenerate. The lower eigenvalues of SDWPs had been calculated in [33] to a high accuracy by using again the Dirichlet boundary value problem on $x \in [-L, L]$. Following the main argument in [33], we first determine a *critical value* of L, which represents *infinity* in the computational sense, and use the resulting eigenvalues as the input of our algorithm in the inverse problem. Unfortunately, we observe that the algorithm is much more sensitive to the initial potential $q^0(x)$ for an SDWP. Actually, satisfactory results could only be reached when $\kappa_1 \approx 0.65$.

The relative potential errors and eigenvalue residuals are listed in Table 5. As in the harmonic oscillator case, Newton's method converges linearly, see Figure 4(a). Finally, the reconstructed SDWP is shown in Figure 4(b).

5. Concluding remarks

In this article, we present an algorithm to solve inverse SLPs on $x \in [-L, L]$ for a symmetric potential $q(-x) = q(x)$ from a knowledge of one sequence of eigenvalues. However, in our specific examples, we make use of the spectra of the corresponding singular problems on $x \in (-\infty, \infty)$. Therefore, our objective is to find an appropriate L, just as in the direct problem, at which the singular potentials may be approximated to a satisfactory accuracy. For sufficiently small values of the boundary parameter, for about 2–3, the algorithm behaves indeed regularly in the sense that the problem seems to be well-posed. However, the singularity can in principle be tackled for increasing L, leading to an ill-posed problem in the sense that a rapid growth of the condition number of the Jacobian is encountered in the use of Newton's method after discretization, which needs a regularization process.

On the other hand, it is not possible to increase L arbitrarily due to the fact that the basis functions (10) in FPM do not characterize the true asymptotic behaviour of the solutions of the singular problem as $x \to \infty$. To be specific, the harmonic oscillator eigenfunctions, for example, behave like $e^{-x^2/2}$ at infinity. Clearly, our basis functions and, hence, the trial solution in Equation (14) is far away from imitating such an exponential behaviour. This reflects the typical property of an asymptotic convergence with respect to L, where a threshold value of which should be determined. Numerical tests show actually that our algorithm incorporated with regularizations provides satisfactory results when L is about 10 and 5.5 for the harmonic oscillator and the SDWP, respectively.

We observe in the case of harmonic oscillator, for example, that as L increases from 7 to 10, the better converged results could be obtained at the cost of a higher number M of input eigenvalues, which is not surprising. In [16], the authors analysed the challenging question of whether the solution of a regular inverse SLP converges to the exact potential function as M tends to ∞. Unfortunately, a similar theoretical analysis seems to be extremely difficult in our case since the problem is ill-posed with almost a singular Jacobian matrix, when L is beyond a certain size.

Acknowledgements

This research was supported by a grant from TUBITAK, the Scientific and Technical Research Council of Turkey.

References

[1] L. Aceto, P. Ghelardoni, and C. Magherini, *Boundary value methods for the reconstruction of Sturm–Liouville potentials*, Appl. Math. Comput. 219(6) (2012), pp. 2960–2974.
[2] A.L. Andrew, *Numerical solution of inverse Sturm–Liouville problems*, ANZIAM J. 45(E) (2004), pp. C326–C337
[3] A.L. Andrew, *Numerov's method for inverse Sturm–Liouville problems*, Inverse Probl. 21 (2005), pp. 223–238.

[4] A.L. Andrew, *Computing Sturm–Liouville potentials from two spectra*, Inverse Probl. 22 (2006), pp. 2069–2081.
[5] P.B. Bailey, W.N. Everitt, and A. Zettl, *Computing eigenvalues of singular Sturm–Liouville problems*, Results Math. 20 (1991), pp. 391–423.
[6] C. Böckmann and A. Kammanee, *Broyden method for inverse non-symmetric Sturm–Liouville problems*, BIT 51 (2011), pp. 513–528.
[7] G. Borg, *Eine Umkehrung der Sturm–Liouvilleschen Eigenwertaufgabe*, Acta Math. 78 (1946), pp. 1–96.
[8] J.P. Boyd, *Chebyshev and Fourier Spectral Methods*, Dover Publications, New York, 2001.
[9] B.M. Brown, V.S. Samko, I.W. Knowles, and M. Marletta, *Inverse spectral problem for the Sturm–Liouville equation*, Inverse Probl. 19 (2003), pp. 235–252.
[10] K. Chadan, D. Colton, L. Päivärinta, and W. Rundell, *An Introduction to Inverse Scattering and Inverse Spectral Problems*, SIAM, Philadelphia, 1997.
[11] M.T. Chu and G.H. Golub, *Inverse Eigenvalue Problems*, Oxford University Press, New York, 2005.
[12] P. Deuflhard, *Newton Methods for Nonlinear Problems: Affine Invariance and Adaptive Algorithms*, Springer-Verlag, Berlin, 2004.
[13] A. Doicu, F. Schreier, and M. Hess, *Iteratively regularized Gauss-Newton method for atmospheric remote sensing*, Comput. Phys. Comm. 148 (2002), pp. 214–226.
[14] H.W. Engl, M. Hanke, and A. Neubauer, *Regularization of inverse problems in Mathematics and its Applications*, Vol. 375, Kluwer Academic Publishers, Dordrecht, Boston, London, 1996.
[15] D. Funaro, *Polynomial Approximation of Differential Equations*, Springer Verlag, Berlin, 1992.
[16] Q. Gao, X. Cheng, and Z. Huang, *On a boundary value method for computing Sturm–Liouville potentials from two spectra*, Int. J. Comput. Math. (to appear, doi:10.1080/00207160.2013.790535).
[17] I.M. Gel'fand and B.M. Levitan, *On the determination of a differential equation from its spectral function*, Amer. Math. Soc. Transl. 1 (1955), pp. 253–305.
[18] P. Ghelardoni and C. Magherini, *BVMs for computing Sturm–Liouville symmetric potentials*, Appl. Math. Comput. 217 (2010), pp. 3032–3045.
[19] P.C. Hansen, and D.P. O'Leary, *The use of the L-curve in the regularization of discrete Ill-posed problems*, SIAM J. Sci. Comput. 14 (1993), pp. 1487–1503.
[20] B. Kaltenbacher, *Some Newton-type methods for the regularization of nonlinear ill-posed problems*, Inverse Probl. 13 (1997), pp. 729–753.
[21] A. Kammanee and C. Böckmann, *Determination of partially known Sturm–Liouville potentials*, Appl. Math. Comput. 204 (2008), pp. 928–937.
[22] A. Kammanee and C. Böckmann, *Boundary value method for inverse Sturm–Liouville problems*, Appl. Math. Comput. 214 (2009), pp. 342–352.
[23] M. Plum, *Eigenvalue problems for differential equations*, in *Wavelets, Multilevel Methods and Elliptic PDE's*, M. Ainsworth, J. Levesley, W.A. Light, and M. Marletta, eds., Clarendon Press, Oxford, 1997, pp. 39–83.
[24] S. Pruess and C.T. Fulton, *Mathematical software for Sturm–Liouville problems*, ACM Trans. Math. Software 19 (1993), pp. 360–376.
[25] J.D. Pryce, *Numerical Solution of Sturm–Liouville Problems*, Oxford University Press, Oxford, 1993.
[26] J.D. Pryce and M. Marletta, *Automatic solution of Sturm–Liouville problems using the Pruess method*, J. Comput. Appl. Math. 39 (1992), pp. 57–78.
[27] M. Rafler and C. Böckmann, *Reconstruction method for inverse Sturm–Liouville problems with discontinuous potentials*, Inverse Probl. 23 (2007), pp. 933–946.
[28] A. Rieder, *On the regularization of nonlinear ill-posed problems via inexact Newton iterations*, Inverse Probl. 15 (1999), pp. 309–327.
[29] A. Rieder, *On convergence rates of inexact Newton regularizations*, Numer. Math. 88 (2001), pp. 347–356.
[30] N. Röhrl, *A least-squares functional for solving inverse Sturm–Liouville problems*, Inverse Probl. 21 (2005), pp. 2009–2017.
[31] W. Rundell and P.E. Sacks, *Reconstruction techniques for classical inverse Sturm–Liouville problems*, Math. Comput. 58 (1992), pp. 161–183.
[32] H. Taşeli, *The influence of the boundedness of polynomial potentials on the spectrum of the Schrödinger equation*, J. Comput. Phys. 101 (1992), pp. 252–255.
[33] H. Taşeli, *Accurate computation of the energy spectrum for potentials with multiminima*, Int. J. Quantum Chem. 46 (1993), pp. 319–334.
[34] H. Taşeli, *Accurate numerical bounds for the spectral points of singular Sturm–Liouville problems over* $-\infty < x < \infty$, J. Comput. Appl. Math. 115 (2000), pp. 535–546.
[35] H. Taşeli and H. Alıcı, *The scaled Hermite–Weber basis in the spectral and pseudospectral pictures*, J. Math. Chem. 38 (2005), pp. 367–378.
[36] C.R. Vogel, *Computational Methods for Inverse Problems*, SIAM, Philadelphia, 2002.
[37] J.A.C. Weidemann and S.C. Reddy, *A MATLAB differentiation matrix suit*, ACM Trans. Math. Softw. 26 (2000), pp. 465–519.
[38] X. Zhang, *Mapped barycentric Chebyshev differentiation matrix method for the solution of regular Sturm–Liouville problems*, Appl. Math. Comput. 217 (2010), pp. 2266–2276.